Mid-infrared lightly Er^{3+}-doped CaF_2 laser under acousto–optical modulation

Yuan-Hao Zhao(赵元昊)[1,†], Meng-Yu Zong(宗梦雨)[1,†], Jia-Hao Dong(董佳昊)[1], Zhen Zhang(张振)[2], Jing-Jing Liu(刘晶晶)[1,‡], Jie Liu(刘杰)[1,§], and Liang-Bi Su(苏良碧)[2]

[1] *Shandong Provincial Engineering and Technical Center of Light Manipulations & Shandong Provincial Key Laboratory of Optics and Photonic Device, School of Physics and Electronics, Shandong Normal University, Ji'nan* 250358, *China*

[2] *State Key Laboratory of High Performance Ceramics and Superfine Microstructure, Shanghai Institute of Ceramics, Chinese Academy of Sciences, Shanghai* 201899, *China*

(Received 27 September 2022; revised manuscript received 14 November 2022; accepted manuscript online 22 November 2022)

A 1.7-at.% Er:CaF_2 crystal was synthesized by temperature gradient method. The Er:CaF_2 crystal was applied in acousto-optically Q-switched laser at mid-infrared region for the first time. Using a TeO_2-based crystal as *Q*-switcher, we obtained a laser diode (LD) end-pumped Er:CaF_2 laser with the highest single pulse energy up to 0.49 mJ and maximum peak power of 0.56 kW under 6.34-W absorbed pump power. The implication of these results is that the low-doped Er:CaF_2 crystal exhibits promising optical properties in solid-state lasers.

Keywords: mid-infrared laser, Er:CaF_2 laser, acousto–optical modulation

PACS: 42.55.Xi, 42.60.Gd, 42.60.Pk **DOI:** 10.1088/1674-1056/aca4c0

1. Introduction

Mid-infrared lasers have received enormous attention for exceptional characteristics, and exhibit applications in multiple areas: remote sensing, laser surgery, and material processing, *etc*.[1,2] Laser at 3 μm coincides with strong absorption of water[3] and it can be utilized as ideal laser source for medical surgery with small penetration depth, low thermal damage, and high action accuracy.[4] For now, two common methods are used to acquire 3-μm laser: nonlinear frequency transformation technique (NFTT), and direct generation.[5] Generally speaking, the transition from $^4I_{11/2}$ level to $^4I_{13/2}$ level of Er^{3+} ions is deemed as a proven method to obtain 2.8-μm laser.[6,7] Structurally, the direct generation method, compared with the other way NFTT, is much simpler. Besides low cost, direct generation approach can also take the advantage of commercial laser diode (LD). To date, the majority of studies on Er^{3+}-doped lasers are largely based on Er:YAG,[8] Er:YSGG,[9,10] Er:GGG,[11] Er:CaF_2,[6] Er:SrF_2,[12] *etc*. To reduce the adverse effects of self-terminating transition, co-doped with deactivated ions or heavily Er^{3+}-doped laser crystals are more inclined to be explored.[13,14] Among them, the heavily doped Er:YAG crystals are the most representative one and the doping concentration generally ranges from 30 at.% to 50 at.%, while it can lead to a sequence of concerns: more inappropriate lifetime ratio between the upper and lower levels, significant degradation of crystal quality, and severe thermal effect, *etc*. Based on CaF_2 being gain medium matrix, lasers with great performance can still be obtained at low concentrations of Er^{3+} ions, thanks to small thermal expansion, high thermal conductivity [about 10 (W/m)/K], lower phonon energy (CaF_2: 322 cm^{-1}, Lu_2O_3: 618 cm^{-1}, Y_2O_3: 579 cm^{-1}, YAG: 875 cm^{-1}, YSGG: 740 cm^{-1}), and characteristic fluorite structure with cluster effect.[15–17] Er:CaF_2 crystals, therefore, can be deemed as promising matrix materials.

The *Q*-switching is a key method to acquire pulsed laser with high energy, for which different techniques have been explored.[18–20] Compared with active *Q*-switching, passive *Q*-switching largely depends on saturable absorbers (SAs) whose modulated parameters are beyond manual control, resulting in low pulse energy and unstable repetition rate. Active *Q*-switching has been done through diverse types of mechanical devices, containing rotating mirrors, prisms, electro–optical (EO) crystals,[21,22] and acousto–optical (AO) crystals.[23] The rotating mirror *Q*-switched laser has complex structure and poor *Q*-switched stability and the EO *Q*-switched laser needs a pretty high voltage circuit of several thousand volts. By contrast, the AOQS laser owns a simple structure and does not need high voltage. Adopting the AO modulation method, the pulsed properties of Er:Y_2O_3 ceramic[24] and Er:CaF_2-SrF_2 crystal[25] have been respectively characterized. For acousto-optically *Q*-switched (AOQS) study, the article, using Er:CaF_2 crystal as gain medium, has not been reported yet.

The activation ions have a decisive influence on the absorption of the pump light and, therefore, are closely related to the amount of heat generated in the medium. The higher the

[†]These authors contributed equally to this work.
[‡]Corresponding author. E-mail: jingjingliu@sdnu.edu.cn
[§]Corresponding author. E-mail: jieliu@sdnu.edu.cn

© 2023 Chinese Physical Society and IOP Publishing Ltd

doping concentration is, the larger the absorption efficiency is, and the faster the pump light intensity decreases in the crystal. Yet, as the doping concentration drops, the distribution of the pump light in the crystal becomes more uniform and crystal heat dissipation effect is better, more conducive to obtain higher output power. Hence, the continuous investigation into the design and growth of gain medium with more suitable ion doping concentration will be of considerable help to the thermal effect of the laser as well as the laser efficiency, further advancing the development of mid-infrared lasers. In the prior work of our group, the low-doped 1.7-at.% Er:CaF_2 laser has been successful in achieving the 2.32-W highest continuous wave output power among LD pumped Er^{3+}-doped fluoride crystals lasers[26] and displays outstanding optical capabilities.

In this letter, using the 1.7-at.% Er:CaF_2 crystal as gain medium, we obtained a stable pulsed laser with high single pulse energy of 0.49 mJ, modulated by a commercial TeO_2-based AO Q-switcher. We, for the first time, demonstrated the AO modulation phenomena of Er:CaF_2 crystal in mid-infrared region in great detail as far as we know.

2. Experimental setup

The Er:CaF_2 crystal with a doping concentration of only 1.7 at.% has been successfully grown by temperature gradient technique which is favorable to the improvement of the thermal loads. The crystal is cut into 3 mm×3 mm in cross section and 12-mm long. Both ends are polished with no coating. The spectral features (absorption spectrum and emission spectrum) have been well documented in earlier work.[26] The experimental setup is depicted in the diagram in Fig. 1. The pumping source is an LD with center wavelength of 980 nm, corresponding to a fiber core size of 400 μm. We adopt the method of LD single-end-pumping, in order to construct a laser with simple structure, good beam quality and good spatial mode. The pumping light is focused on the crystal middle through a 1:1 coupling system and the spot radius at crystal position is approximately 200 μm. The crystal is tightly wrapped by thin indium foil and mounted into the copper heatsink which is equipped with circulating water whose temperature is constant 12 °C. The absorption efficiency of the laser crystal is 56.9%. M_1, a plane mirror, and M_2, a concave mirror with curvature of 100 mm are both coated with anti-reflexivity at 974 nm and high reflexivity at 2.7 μm–2.95 μm. M_3, an output coupler (OC), is partial-reflectively coated and shows a transmission around 2.7 μm–2.95 μm of 5%.

A TeO_2-based AO Q-switcher (No: I-QS041-1.5C2P, Gooch company) is placed in the cavity, close to the OC. The rising time and the active aperture of the AO crystal are 153 ns/mm and 1.5 mm. The Q-switcher has high transmittance of more than 95%, coated from 2.8 μm to 3 μm on two ends and the maximum radio-frequency power of the power driving is up to 10 W at the frequency of 40.68 MHz.

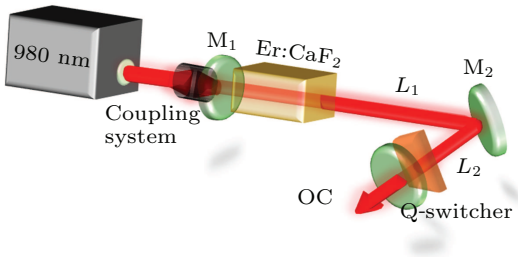


Fig. 1. Schematic diagram of the AOQS Er:CaF_2 laser (L_1 = 81 mm, L_2 = 111 mm).

3. Results and discussion

In the continues wave (CW) operation mode, the Er:CaF_2 laser without AO Q-switcher is reaped with 0.83-W maximum output power and slope efficiency of 10%, as measured with a laser power meter (30A-SH-V1, Israel) shown in Fig. 2(a). While the absorbed pump power exceeds 1.04 W, the CW laser begins to oscillate. The AOQS laser threshold of 4.01 W is much higher than that of CW laser, which is mainly caused by the insertion loss of the AO modulation device. As shown in Fig. 2(b), the spectrum of the CW Er:CaF_2 laser, recorded with a spectrum analyzer (SOL-MS3504i), reveals that the peak of the emitted central spectrum is located at 2756.8 nm with full width at half maximum (FWHM) of 1 nm, nonlinear fitted by Gaussian function.

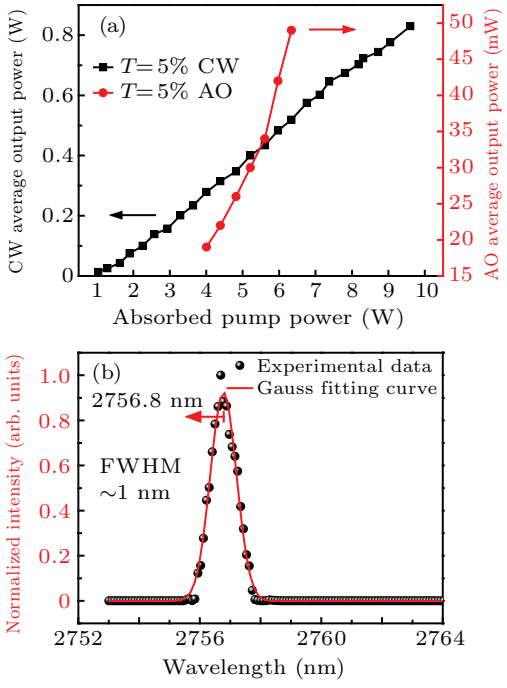


Fig. 2. (a) Average output power *versus* absorbed pump power for CW and AOQS lasers. (b) Output spectrum of CW Er:CaF_2 laser.

In the AO region, variations of the main parameters in relation to the absorbed pump power are displayed in Fig. 2(a) and Figs. 3(a)–3(c). The cross-sectional area of the beam is

observed through an MIR detector card and it turns out that the spot profile is regular and circular, which can be seen as operating in TEM_{00} mode. The maximum output power of AOQS laser is 49 mW, corresponding to 6.34-W absorbed pump power at this point. When the absorbed pump power reaches around 6.34 W, the output power does not increase and shows instability. In order to protect the crystal from damage, we do not continue to increase the incident power. We analyze the phenomenon of low output power, which may be due to insertion loss of modulation components and the incomplete match between laser oscillation wavelength and the coating range of AO crystal. The output wavelength is located at 2756.8 nm which belongs to the edge of the range of AO crystal coating wavelength (2.8 μm–3 μm), thus resulting in large energy loss in the laser cavity. Subsequent use of AO crystal with a more suitable coating range is expected to further improve the output power. When the AO modulation device is driven from 100 Hz to 1000 Hz, the shortest pulse durations are 875 ns, 555 ns, and 752 ns, respectively.

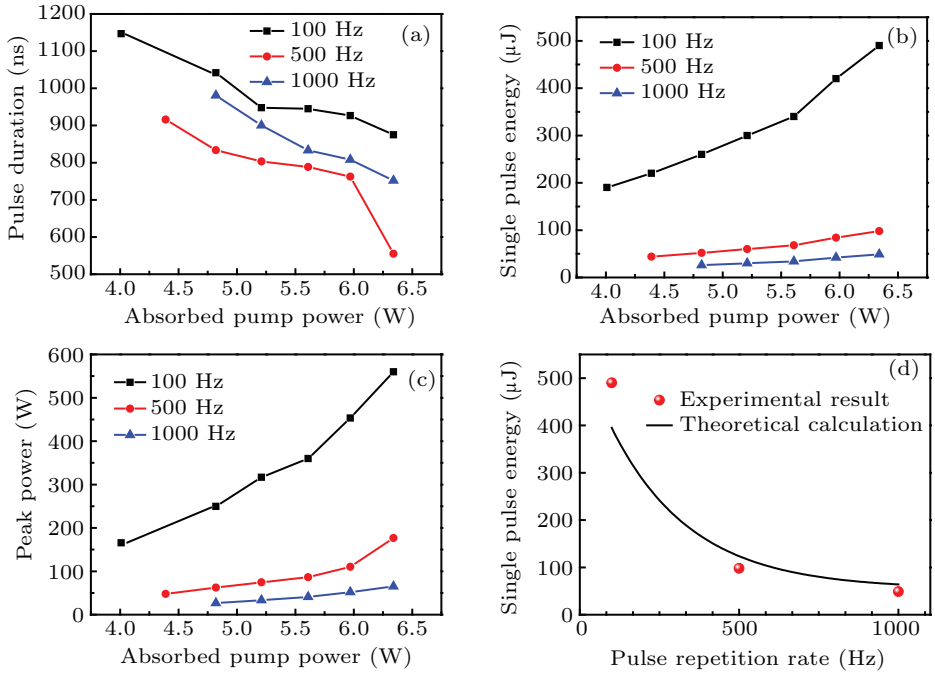


Fig. 3. (a) The pulse duration, (b) single pulse energy, and (c) peak power of AOQS Er:CaF_2 lasers with PRFs of 100 Hz, 500 Hz, and 1000 Hz. (d) Theoretical and actual values of single pulse energies.

The pulse energy is furnished by the stimulated radiation process ($^4I_{11/2}$ state to $^4I_{13/2}$ state) which consumes the count of inverted particles. With the increase of the PRF from 100 Hz to 500 Hz and then 1000 Hz, the accumulation time of upper level particles becomes shorter and the inverted particles can not reach the maximum value, which lead to less energy accumulation inside the laser crystal. Therefore, the single pulse energy decreases significantly from 490 μJ to 98 μJ and then 49 μJ. As for the maximum peak powers, they are calculated to be 560 W, 176.58 W, and 65.16 W respectively. All these data are summarized in Table 1.

Table 1. Performances of the AOQS laser under different pulse repetiton frequencies.

Pulse repetiton frequency (Hz)	Pulse duration (ns)	Single pulse energy (μJ)	Peak power (W)
100	875	490	560
500	555	98	176.58
1000	752	49	65.16

Table 2 summarizes a few available research data relating to LD end-pumped AOQS Er^{3+} lasers at 2.8 μm and there are not many articles involved so far. Compared with other experimental results, the single pulse energy obtained in this work is higher.

Table 2. Comparison of LD end-pumped AOQS Er^{3+} lasers at 2.8 μm.

Gain medium	η (at.%)	Method	E_s (mJ)	Ref.
Er:$Y_2O_3^*$	7	AO	0.3	[24]
Er:CaF_2-SrF_2	3	AO	0.39	[25]
Er:CaF_2	1.7	AO	0.49	this work

η: doping concentration, E_s: single pulse energy, *: ceramic.

Employing the conventional coupled rate equation model, the theoretical value of the single pulse energy, in a *Q*-switched laser, can be calculated using the formula

$$E_P = h\nu(\pi\omega_0^2 l)\frac{\ln(1/R)}{\ln(1/R)+L}(n_i - n_f), \tag{1}$$

where $h\nu$ is the phonon energy of laser, $\pi\omega_0^2 l$ is cavity mode volume, R is the reflectance of OC, L is the energy dissipation in the cavity and n_i, n_t, n_f denote the initial, threshold, and final particle number densities, respectively. The relationship

among n_i, n_t, and n_f is

$$n_i - n_f = n_t \ln \frac{n_i}{n_f}. \tag{2}$$

It is seen that as long as the above three particle number densities can be figured out, then the single pulse energy will be calculated

$$n_t = \frac{1}{2\sigma l}\left[\ln\left(\frac{1}{R}\right) + L\right], \tag{3}$$

$$n_i = R_p \tau\left[1 - \exp\left(\frac{-1}{\tau f}\right)\right] + n_f \exp\left(\frac{-1}{\tau f}\right), \tag{4}$$

$$R_p = \frac{P_{abs}}{h\nu_p \pi \omega_p^2 l}, \tag{5}$$

where σ is the emission cross-section, R_p is the pumping rate, τ is the fluorescence lifetime of upper lever, f is the PRF, P_{abs} is the absorbed pump power, ν_p and ω_p are the frequency and radius of the pumping light. By combining these three equations (3)–(5), we can derive particle number densities which in turn lead to the E_p. In calculations, the required data are given in Table 3. For some non-objective values, we shall need to compare and modify them repeatedly with the experiment itself, and there is bound to exist some degree of error with the actual results within acceptable range. The theoretical single pulse energies at different PRFs are shown follows in Fig. 3(d). The single pulse energies are calculated theoretically and experimentally, which agree well with each other. It can be seen that the theoretical analysis provides a reasonable description of the experimental data and verifies the scientific nature.

Table 3. Required data for calculation.

Parameter	Symbol	Value
Crystal length	l	12 mm
Reflectance	R	0.95
Fluorescence lifetime	τ	7.5 ms
Emission cross-section	σ	6.75×10^{-21} cm^2
Absorbed pump power	P_{abs}	6.34 W

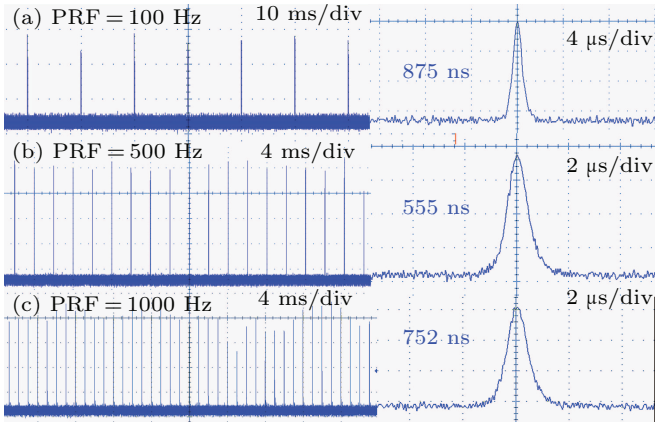


Fig. 4. The AOQS temporal pulse trains: (a) PRF = 100 Hz, 10 ms/div, and 4 μs/div; (b) PRF = 500 Hz, 4 ms/div, and 2 μs/div; (c) PRF = 1000 Hz, 4 ms/div, and 2 μs/div.

The temporal pulse profiles are converted into electrical signal and visualized by the photodetector with rapid response speed (VIGO System S.A. with a rise time of around 3.5 ns) and a digital oscilloscope with bandwidth of 1 GHz (Tektronix DPO4104, 5G samples/s). The stable AO temporal pulse trains recorded at different time scales are exhibited in Fig. 4. Observing the change of pulse image on digital oscilloscope, we can see that the whole pulse train is neat and stable over a period of time.

4. Conclusions

In summary, a lightly-doped Er:CaF_2 crystal was synthesized and we have carried out a specific study on its pulsed laser characteristics. In the CW region, the 1.7-at.% Er:CaF_2 laser with 0.83-W maximum output power is obtained at 2756.8 nm with the FWHM of 1 nm. As for the Er:CaF_2 pulsed laser modulated by AO Q-switcher, the highest single pulse energy, peak power, and shortest pulse duration are 0.49 mJ, 0.56 kW, and 555 ns, respectively. In subsequent experiments, the use of AO crystal with a more suitable coating range will hopefully further improve the phenomenon of low output power. The experimental data manifest that low-doped Er:CaF_2 crystal owns great optical potential as a gain medium in mid-infrared lasers.

Acknowledgements

Project supported by the National Natural Science Foundation of China (Grant Nos. 11974220, 61925508, 61905265, and 12104271), the Natural Science Foundation of Shandong Province, China (Grant Nos. ZR2021LLZ008 and ZR2021QA030), the Fund from Science and Technology Commission of Shanghai Municipality (Grant No. 20511107400), and CAS Interdisciplinary Innovation Team (Grant No. JCTD-2019-12).

References

[1] Chen Y Z, Zhang Q L, He Y, Quan C, Luo J Q, Xu J Y and Sun D L 2020 *Opt. Laser Technol.* **121** 105811
[2] Xue Y Y, Xu X D, Su L B and Xu J 2020 *J. Synth. Cryst.* **49** 1347
[3] Frauchiger J and Lüthy W 1987 *Opt. Quantum Electron.* **19** 231
[4] Hohenleutner U, Hohenleutner S, Bäumler W and Landthaler M 1997 *Lasers Surg. Med.* **20** 242
[5] Peng Y F, Wei X B, Luo X W, Nie Z, Peng J, Wang Y and Shen D Ye 2016 *Opt. Lett.* **41** 49
[6] Basiev T T, Orlovskii Yu V, Polyachenkova M V, Fedorov P P, Kuznetsov S V, Konyushkin V A, Osiko V V, Alimov O K and Dergachev A Y 2006 *Quantum Electron.* **36** 591
[7] Tian Q Y, Yin P, Zhang T, Zhou L B, Xu B, Luo Z Q, Liu H L, Ge Y Q, Zhang J, Liu P and Xu X D 2020 *Nanophotonics* **9** 2495
[8] Huang J H, Wang B, You W X, Zhang L L, Sun Y J, Tu C Y, Gong G L and Liu Y 2021 *Spectrochim. Acta A: Mol. Biomol. Spectrosc.* **258** 119587
[9] Shen B J, Kang H X, Sun D L, Zhang Q L, Yin S T, Chen P and Liang J 2013 *Laser Phys. Lett.* **11** 015002
[10] Arbabzadah E, Chard S, Amrania H, Phillips C and Damzen M 2011 *Opt. Express* **19** 25860

[11] You Z Y, Wang Y, Xu J L, Zhu Z J, Li J F, Wang H Y and Tu C Y 2015 *Opt. Lett.* **40** 3846
[12] Švejkar R, Šulc J, Jelínková H, Kubeček V, Ma W W, Jiang D P, Wu Q H and Su L B 2018 *Opt. Mater. Express* **8** 1025
[13] Wang Y, You Z Y, Li J F, Zhu Z J, Ma E and Tu C Y 2009 *J. Phys. D: Appl. Phys.* **42** 215406
[14] Zhang P X, Li S M, Yang Y L, Zhang L H, Li Z, Chen Z Q and Hang Y 2020 *J. Synth. Cryst.* **49** 1369
[15] Yao W H, Uehara H, Tokita S Chen H J, Konishi D, Murakami M and Yasuhara R 2020 *Appl. Phys. Express* **14** 012001
[16] Ding S J, Ren H, Li H Y and He A F 2021 *J. Mater. Sci. Mater. Electron.* **32** 1616
[17] Ma W W, Su L B, Xu X D, Wang J Y, Jiang D P, Zheng L H, Fan X W, Li C, Liu J and Xu J 2016 *Opt. Mater. Express* **6** 409
[18] Zhang F, Zhang H N, Liu D H, Liu J, Ma F K, Jiang D P Pang S Y, Su L B and Xu J 2017 *Chin. Phys. B* **26** 024205
[19] Zhao Y H, Zong M Y, Zheng J, Zhang Z, Peng Q Q, Jiang S Z, Liu J, Liu J J and Su L B 2022 *Nanomaterials* **12** 454
[20] Maleki A, Kavosh Tehrani M, Saghafifar H and Moghtader Dindarlu M H 2016 *Chin. Phys. B* **25** 034206
[21] Ma S H, Lu D Z, Yu H H, Zhang H J, Han X K, Lu Q M, Ma C Q and Wang J Y 2017 *Opt. Express* **25** 24007
[22] Yang Z X, Zaheer U D S, Wang P C, Li C, Lin Z W, Leng J C, Liu J, Xu L, Yang Q and Ren X H 2022 *Opt. Laser Technol.* **148** 107711
[23] Chen X W, Xu H H, Guo Y F, Han W J, Yu H H, Zhang H J and Liu J H 2015 *Appl. Opt.* **54** 7142
[24] Ren X J, Wang Y F, Fan X L, Zhang J, Tang D Y and Shen D Y 2017 *IEEE Photon. J.* **9** 15004306
[25] Liu J J, Zong M Y, Wang D Z, Zhang Z, Liu J and Su L B 2021 *Infrared Phys. Technol.* **116** 103758
[26] Zong M Y, Wang Y F Zhang Z, Liu J J, Zhao L N, Liu J and Su L B 2022 *J. Lumin.* **250** 119089